Journal of Molecular and Cellular Cardiology 88 (2015) 39–54

Contents lists available at ScienceDirect

Journal of Molecular and Cellular Cardiology

journal homepage: www.elsevier.com/locate/yjmcc

p63RhoGEF regulates auto- and paracrine signaling in cardiac fibroblasts

Anita Ongherth [a,d,1], Sebastian Pasch [a,d,1], Christina M. Wuertz [a,d], Karolin Nowak [a], Naim Kittana [a,d], Cleo A. Weis [b], Aline Jatho [a,d], Christiane Vettel [a,b,d], Malte Tiburcy [a,d], Karl Toischer [c,d], Gerd Hasenfuss [c,d], Wolfram-Hubertus Zimmermann [a,d], Thomas Wieland [b,d], Susanne Lutz [a,d,*]

[a] Institute of Pharmacology, Medical Center Goettingen, Germany
[b] Institute of Experimental and Clinical Pharmacology and Toxicology, Medical Faculty Mannheim, University of Heidelberg, Germany
[c] Department of Cardiology and Pneumology, Medical Center Goettingen, Germany
[d] DZHK (German Center for Cardiovascular Research) partner sites Goettingen and Mannheim, Germany

ARTICLE INFO

Article history:
Received 18 February 2015
Received in revised form 4 September 2015
Accepted 16 September 2015
Available online 21 September 2015

Keywords:
Cardiac remodeling
p63RhoGEF
RhoA
Connective tissue growth factor

ABSTRACT

Cardiac remodeling, a hallmark of heart disease, is associated with intense auto- and paracrine signaling leading to cardiac fibrosis. We hypothesized that the specific mediator of $G_{q/11}$-dependent RhoA activation p63RhoGEF, which is expressed in cardiac fibroblasts, plays a role in the underlying processes. We could show that p63RhoGEF is up-regulated in mouse hearts subjected to transverse aortic constriction (TAC). In an engineered heart muscle model (EHM), p63RhoGEF expression in cardiac fibroblasts increased resting and twitch tensions, and the dominant negative p63ΔN decreased both. In an engineered connective tissue model (ECT), p63RhoGEF increased tissue stiffness and its knockdown as well as p63ΔN reduced stiffness. In 2D cultures of neonatal rat cardiac fibroblasts, p63RhoGEF regulated the angiotensin II (Ang II)-dependent RhoA activation, the activation of the serum response factor, and the expression and secretion of the connective tissue growth factor (CTGF). All these processes were inhibited by the knockdown of p63RhoGEF or by p63ΔN likely based on their negative influence on the actin cytoskeleton. Moreover, we show that p63RhoGEF also regulates CTGF in engineered tissues and correlates with it in the TAC model. Finally, confocal studies revealed a closely related localization of p63RhoGEF and CTGF in the trans-Golgi network.

1. Introduction

During heart disease the myocardium undergoes dramatic structural changes. This involves not only hypertrophic growth and cardiomyocyte loss, but also abundant deposition of extracellular matrix (ECM) in the interstitial and perivascular regions of the heart. This fibrotic process is accompanied by an increase in myocardial stiffness and deterioration of its contractile function [1,2]. Unlike the intensively investigated molecular mechanisms which are responsible for cardiomyocyte dysfunction in the diseased heart, processes leading to cardiac fibrosis are less defined. Several factors have been attributed to play a major role, e.g. the transforming growth factor β (TGF-β) [3,4] and the matricellular protein connective tissue growth factor (CTGF), which are both mechanistically interconnected [5]. In case of CTGF a consistent upregulation was found in the diseased human heart and in several mouse models displaying cardiac fibrosis [6]. Therefore, CTGF is nowadays accepted as a marker for diverse fibrotic diseases, including heart failure.

CTGF is a cysteine-rich, matrix-associated, heparin-binding factor which does not possess a receptor in a classical sense [7]. It contains several potential binding modules for other growth factors, like TGF-β, bone morphogenetic proteins (BMPs), and insulin-like and vascular endothelial growth factors. By anchoring to the ECM, CTGF is thought to coordinate the micro-milieu in the myocardium by keeping diverse growth factors in close vicinity to cardiac cells and their receptors. However, in vivo data on the role of CTGF are surprisingly conflicting ranging from a pro-fibrotic to a cardiomyocyte protective function [8–11]. Similar to the still obscure role of CTGF, there is not much data available how the regulation of CTGF expression and secretion is achieved in cardiac cells. There is, however, evidence that CTGF is regulated via G protein-coupled receptor activation, and angiotensin II (Ang II) as well as endothelin-1 (ET-1) have been implicated in this process [12–16]. With respect to downstream signaling a role of the actin cytoskeleton regulator RhoA and the serum response factor has been postulated [17,18].

The RhoA activator p63RhoGEF has been firstly discovered by Souchet and co-workers in 2001 [19]. Its transcript could be predominately detected in human brain and heart tissue and with respect to cardiomyocytes the authors showed that it is presumably localized close to the sarcomeric I-band. They further provided first evidence that p63RhoGEF functions as a specific guanine nucleotide exchange

* Corresponding author at: Institute of Pharmacology, University of Goettingen, Robert-Koch-Str. 40, 37075 Goettingen, Germany.
E-mail address: Susanne.Lutz@med.uni-goettingen.de (S. Lutz).
[1] These authors contributed equally.

http://dx.doi.org/10.1016/j.yjmcc.2015.09.009
0022-2828/

factor for RhoA, which could be confirmed by several other groups. We identified $G\alpha_{q/11}$ proteins as specific and exclusive upstream activators of p63RhoGEF [20,21]. Subsequently, we were able by loss-of-function studies to demonstrate that p63RhoGEF mediates the Ang II-dependent RhoA activation in aortic smooth muscle cells and is involved in their contraction as well as proliferation [22]. This knowledge was further extended by studies showing that ET-1 mediates its contractile effects on smooth muscle cells via p63RhoGEF [23]. So far little is known about the role of the p63RhoGEF-dependent RhoA activation in the heart. We therefore analyzed the involvement of p63RhoGEF in GPCR-dependent signaling and processes [24]. Specifically, we asked whether activation of the $G\alpha_{q/11}$-p63RhoGEF-RhoA cascade is involved in the regulation of CTGF as well as in auto- and paracrine processes in cardiac fibroblasts.

2. Materials and methods

2.1. Material

All reagents used for cell culture were purchased from Life technologies unless otherwise indicated. Cells were grown in a humidified incubator with 5% CO_2 at 37 °C. All reagents were of the highest quality available and obtained from commercial sources. The following compounds were used: angiotensin II (Ang II, 100 nM, Sigma-Aldrich), endothelin-1 (ET-1, 100 nM, Sigma-Aldrich), phenylephrine (PE, 10 μM Sigma-Aldrich), latrunculin A (LatA, 8.5 μM, Cayman), fasudil (10 μg/ml, LKT Laboratories), H1152 (300 nM, Cayman), C3T (1 μg/ml, Cytoskeleton), CCG1423 (10 μM, Santa Cruz). For fluorescence labeling of actin filaments TRITC-or FITC-phalloidin from Sigma-Aldrich and for indirect labeling of the Golgi apparatus AlexFluor488-wheat germ agglutinin (WGA) from Life Technologies was used. DAPI was obtained from Sigma-Aldrich. All cell culture media were obtained from Gibco Life technologies.

2.2. Mouse heart tissue for protein expression analysis

For the protein expression analysis of p63RhoGEF and CTGF in sham and transverse aortic constriction (TAC) operated female mice, tissues from an already published study by Toischer and colleagues were used [25]. The exact details can be found in this publication.

2.3. Animal studies

Animal care and mouse experiments were carried out in accordance with the guidelines of the institutional animal care and use committee (LAVES, Germany). Mice were kept on a 12 h light/dark cycle with water and food ad libitum.

Ten-to-twelve-weeks-old male and female mice (mixed C57BLJ/6x129S1/SvImJ background) underwent TAC or sham surgery. Therefore, mice were anesthetized by intraperitoneal injection of Medetomidin (0.5 mg/kg) and Midazolam (5 mg/kg), for pain relief Fentanyl (0.05 mg/kg) was injected. The aortic arch was exposed via median thoracotomy and a constriction between the first and second left carotid artery was created using a 6–0 suture and tied against a 27-gauge needle. Sham surgeries were performed in the same way, however, without constriction of the aorta. As antagonizing narcotics Atipamezol (2.5 mg/kg) and Flumazenil (0.5 mg/kg) and for post-procedural pain relief Buprenorphin (0.05–0.1 mg/kg) were injected subcutaneously. In addition, all animals received Metamizol for pain relief in the drinking water over a time period of 2 d before until 7 d after surgery.

Echocardiography measurements were performed before and 1, 3 and 5 weeks after TAC or sham surgery under isoflurane anesthesia (1%) with a Vevo2100 system (Vevo). Transverse aortic flow velocities were obtained 3 d after the surgery and pressure gradients were calculated.

At the end of the study, animals were sacrificed by cervical dislocation and hearts quickly excised for further processing.

2.4. Generation of recombinant adenoviruses

Recombinant adenovirus was generated according to the method published by He and co-workers [26]. The cloned sequences are: human p63RhoGEF aa 1–580 (human Ad-p63RhoGEF) and human p63RhoGEF aa 295–580 (Ad-p63ΔN) both containing an additional N-terminal c-Myc-tag, human PDZ-RhoGEF aa 266–485 (Ad-PRG-RGS) and mouse Lsc aa 1–245 (Ad-RGS-Lsc). For overexpression of p63RhoGEF-specific shRNA (Ad-shp63, specific si-sequence: 5′-GTGG TGTACTGCCAGAATA-3′) a modified pAdTrack vector with an H1-promotor was used [27]. All viruses encode in addition for the enhanced green fluorescent protein (EGFP). Ad-shEGFP virus was a kind gift from F. Cuello, Hamburg, Germany coding for EGFP and a shRNA against EGFP under control of the H1 promoter.

2.5. Isolation and culture of neonatal rat cardiac cells and neonatal rat cardiac fibroblasts (NRCFs)

Cardiac fibroblasts were isolated from neonatal Wistar rats (d 0 to 3) by using a modified cell isolation protocol established by Webster et al. [28]. In brief, the atria of the isolated hearts were removed, the ventricular tissues cut in pieces and washed with CBFHH (0.14 M NaCl, 5.4 mM KCl, 0.81 mM $MgSO_4$, 0.44 mM $KHPO_4$, 0.34 mM Na_2HPO_4, 5.6 mM Glucose, 20 mM HEPES). Next, the tissue was dissociated by alternating incubation in trypsin and DNAseI solutions in CBFHH at room temperature while continuously shaking and gentle pipetting, respectively. The first supernatant was discarded, the followings were collected and the digest was stopped by adding fetal calf serum (FCS). After centrifugation for 15 min at 60 g and 4 °C, the cells were pooled, washed with ice-cold DMEM containing 10% FCS and antibiotics and then filtered through a 250 μm mesh. The filtered cells were either used directly for EHM preparation or incubated for 60 min at 37 °C, 5% CO_2 on a cell culture plate at a density of 10^6 cells per 145 cm^2. Afterwards, the non-attached cardiomyocytes were removed and the attached cardiac fibroblasts were further cultivated in DMEM, 10% FCS, 1% antibiotics, 1% non-essential amino acids, (NEAA) until confluency was reached. Only passage 1 or 2 (P1 or P2) NRCFs were used for the experiments. As assessed by microscopy the number of cardiomyocytes in culture was less than 5%.

2.6. Preparation and measurement of engineered heart muscle (EHM)

EHMs were prepared and measured as described before [29,30] either by using 2.5×10^6 freshly isolated total heart cells for direct transduction or a mixture of 2.5×10^6 total heart cells plus 0.5×10^6 adenovirally transduced P1 NRCF. In detail, the cells were mixed with collagen type I (0.8 mg in 900 μl, rat tail, self-made), a basement membrane protein mixture (10% *v/v*; Matrigel, BD) and concentrated serum-containing culture medium (2 × DMEM in water, supplemented with 20% horse serum, 4% chick embryo extract (CEE, self-made), 200 U/ml

Fig. 1. p63RhoGEF expression in murine hearts subjected to TAC correlates with CTGF expression, with the left ventricular volumes and the contractile function. A) Samples of mouse hearts 7 d after TAC or sham operation were lysed in GST-Fish buffer. Equal protein amounts were used for immunoblot analysis. Shown are representative immunoblots of p63RhoGEF, CTGF, vimentin and calsequestrin-2 (CSQ). The expression of p63RhoGEF and CTGF were quantified and are given normalized to vimentin and calsequestrin relative to the sham group (means ± SEM n = 6; *p < 0.05 vs. sham). B) Samples of male (M) and female (F) mouse hearts after TAC were used for RNA isolation and qPCR. p63RhoGEF and CTGF expression was normalized with the help of the housekeeping gene PBGD. Given are the normalized and relative values as means ± SEM, n = 4 (sham) and n = 8 (TAC),*p < 0.05 vs. sham. In addition, the correlation between p63RhoGEF and CTGF is depicted. The p and r^2 values are given above the graph. C) p63RhoGEF expression, as analyzed by qPCR, is correlated to the diastolic volume (Vd) and the systolic volume (Vs) (left graph) as well as to the ejection fraction (EF) (right graph) analyzed by echocardiography. The p and r^2 values are given above the graphs.

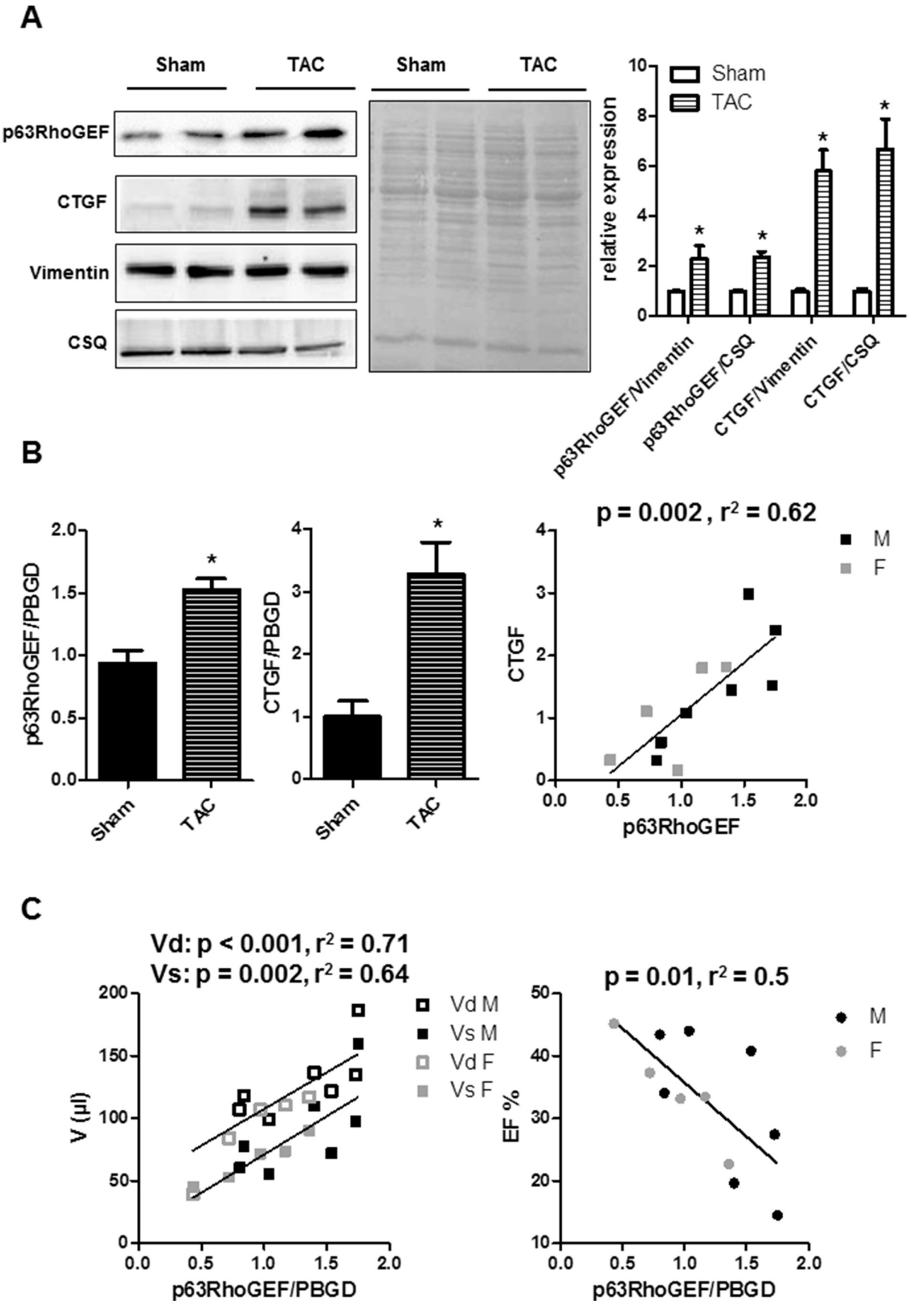
A
Sham
TAC
Sham
TAC
p63RhoGEF
CTGF
Vimentin
CSQ
relative expression
Sham
TAC
p63RhoGEF/Vimentin
p63RhoGEF/CSQ
CTGF/Vimentin
CTGF/CSQ
B
p63RhoGEF/PBGD
CTGF/PBGD
Sham
TAC
p = 0.002 , r² = 0.62
CTGF
p63RhoGEF
M
F
C
Vd: p < 0.001, r² = 0.71
Vs: p = 0.002, r² = 0.64
V (µl)
p63RhoGEF/PBGD
Vd M
Vs M
Vd F
Vs F
p = 0.01, r² = 0.5
EF %
p63RhoGEF/PBGD
M
F

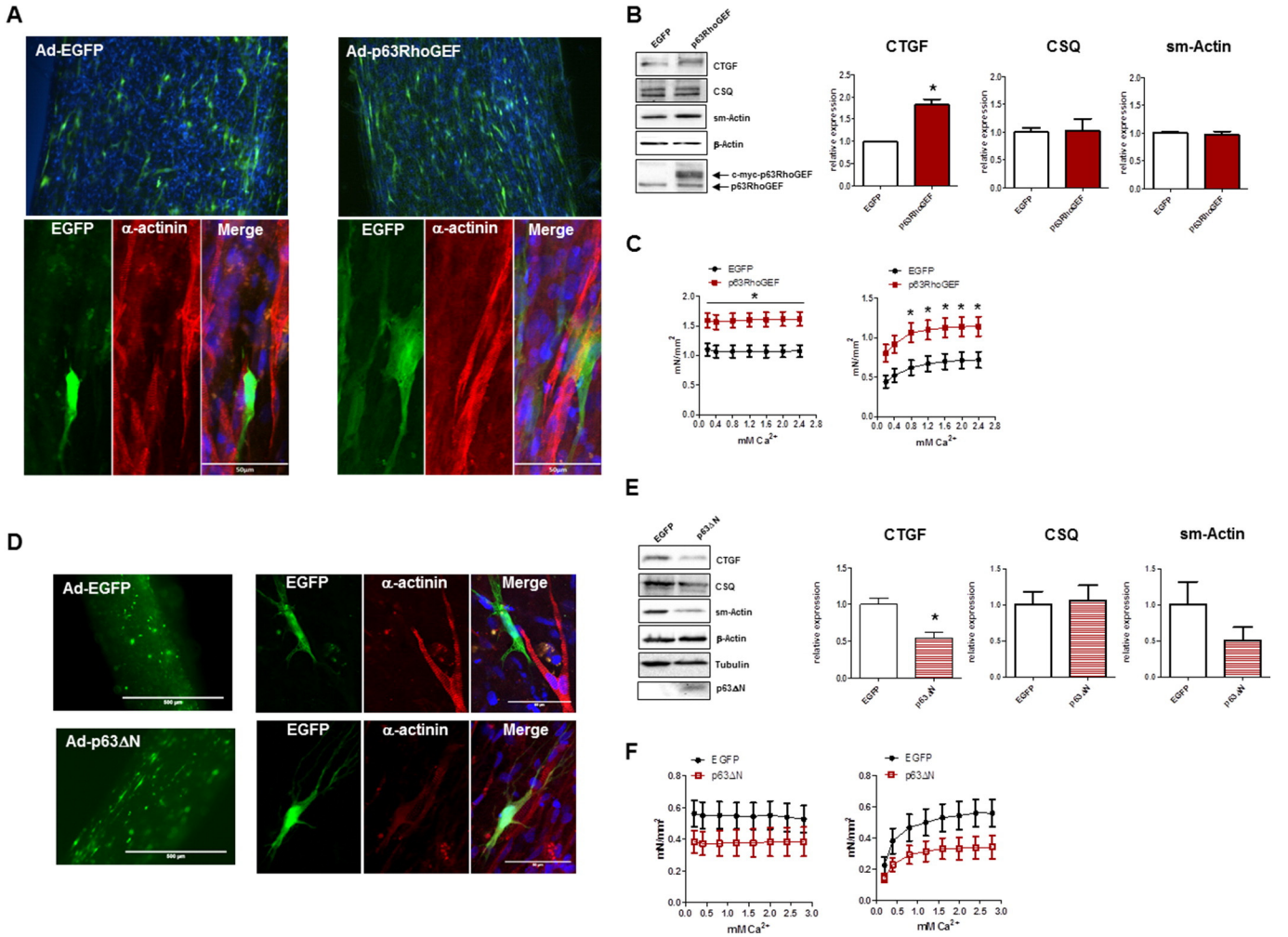

Fig. 2. p63RhoGEF in cardiac fibroblasts influences CTGF expression and contractile function of EHM. NRCFs were transduced with Ad-EGFP (left panels), Ad-p63RhoGEF (right panels) (A–C) or Ad-p63ΔN (D–F) for 24 h and added to cardiac cells for EHM preparation. A, D) EGFP expression was detected in sections of EHM to ensure equal distribution of modified fibroblasts. α-Actinin was stained by immunofluorescence and imaged by confocal microscopy together with EGFP and DAPI. B, E) EHM were homogenized and analyzed by immunoblot with the indicated antibodies. Representative immunoblots are shown. The expression of CTGF, calsequestrin-2 and sm-actin were normalized to β-actin and give relative to the Ad-EGFP-NRCF-containing EHM (EGFP). Values are means ± SEM, *$p < 0.05$ vs. EGFP, $n = 7–10$. C, F) Contraction analysis of EHM. In the left panel the analysis of contractile force normalized to cross sectional area at different calcium concentrations is depicted. In the right panel the resting force normalized to cross sectional area at different calcium concentrations is shown. Shown are means ± SEM, $n = 3–5$, in total 15–20 EHM per group were analyzed per condition, *$p < 0.05$ vs. EGFP.

penicillin, and 200 μg/ml streptomycin, pH adjusted to 7.4 with NaOH). The mixture was cast into circular molds and incubated at 37 °C and 5% CO_2 for 1 h, then filled with DMEM, 10% horse serum, 2% CEE, 100 U/ml penicillin and 100 μg/ml streptomycin (EHM medium). After 24 h the medium was replaced by fresh EHM medium containing for some experiments the Ad-EGFP or Ad-p63RhoGEF adenoviruses (multiplicity of infection 10). Later on, the EHM medium was changed every second day. After 7 d of culture the condensed EHMs were transferred on phasic stretchers and stretched at 1 Hz for 24 h, then at 2 Hz for another 6 d while medium change was continued as described before. Following phasic stretch for 7 to 12 d, the EHMs were transferred to an organ bath at 37 °C containing Tyrode's solution (119.8 mM NaCl, 5.4 mM KCl, 0.2 mM $CaCl_2$, 1.05 mM $MgCl_2$, 0.42 mM NaH_2PO_4, 22.6 mM $NaHCO_3$, 5 mM glucose, 0.28 mM ascorbic acid) and continuously gassed with 95%/5% O_2/CO_2. The EHM were paced with 2 Hz in the presence of a calcium concentration of 1.8 mM and stretched to L_{max}, the length where the maximal force is generated. After buffer change and equilibration the contraction force of EHM was measured under increasing Ca^{2+} concentrations from 0.2 to 3.2 mM. The minimum (diastolic) force was considered as resting force given normalized by the cross sectional area, the difference between the minimum and the maximum force is presented as force of contraction given normalized to the cross sectional area.

For further analysis the EHMs were grinded in liquid nitrogen and homogenized in GST-Fish buffer containing 50 mM Tris pH 7.4, 150 mM NaCl, 4 mM $MgCl_2$, 10% Glycerol (*v*/*v*), 1% Igepal CA-630 (*v*/*v*). After centrifugation (4 °C, 13,000 *g*, 2 min), supernatants were taken for immunoblot analysis. Alternatively, EHMs were fixed in Roti-Histol over

Fig. 3. Influence of p63RhoGEF on CTGF expression and mechanical properties of ECT. NRCFs were transduced with Ad-EGFP, Ad-p63RhoGEF, Ad-p63ΔN for 24 h (A–C) or Ad-EGFP and Ad-shp63 for 72 h (D–F). A, D) Imaging of ECTs and ECT sections. B, E) ECTs were elongated stepwise in an organ bath and force was detected. Given are measured forces per cross sectional area as means ± SEM, *$p < 0.05$ vs. EGFP, $n = 4–5$, 10–22 ECT were measured each. C, F) Stretched (C and F) and unstretched (C) ECTs were minced and lysates were subjected to immunoblot analysis with the respective primary antibodies. Representative immunoblots are shown. Values are means ± SEM, normalized to tubulin and relative to EGFP, $n = 3$ in 2–6 replicates; *$p < 0.05$ vs. EGFP.

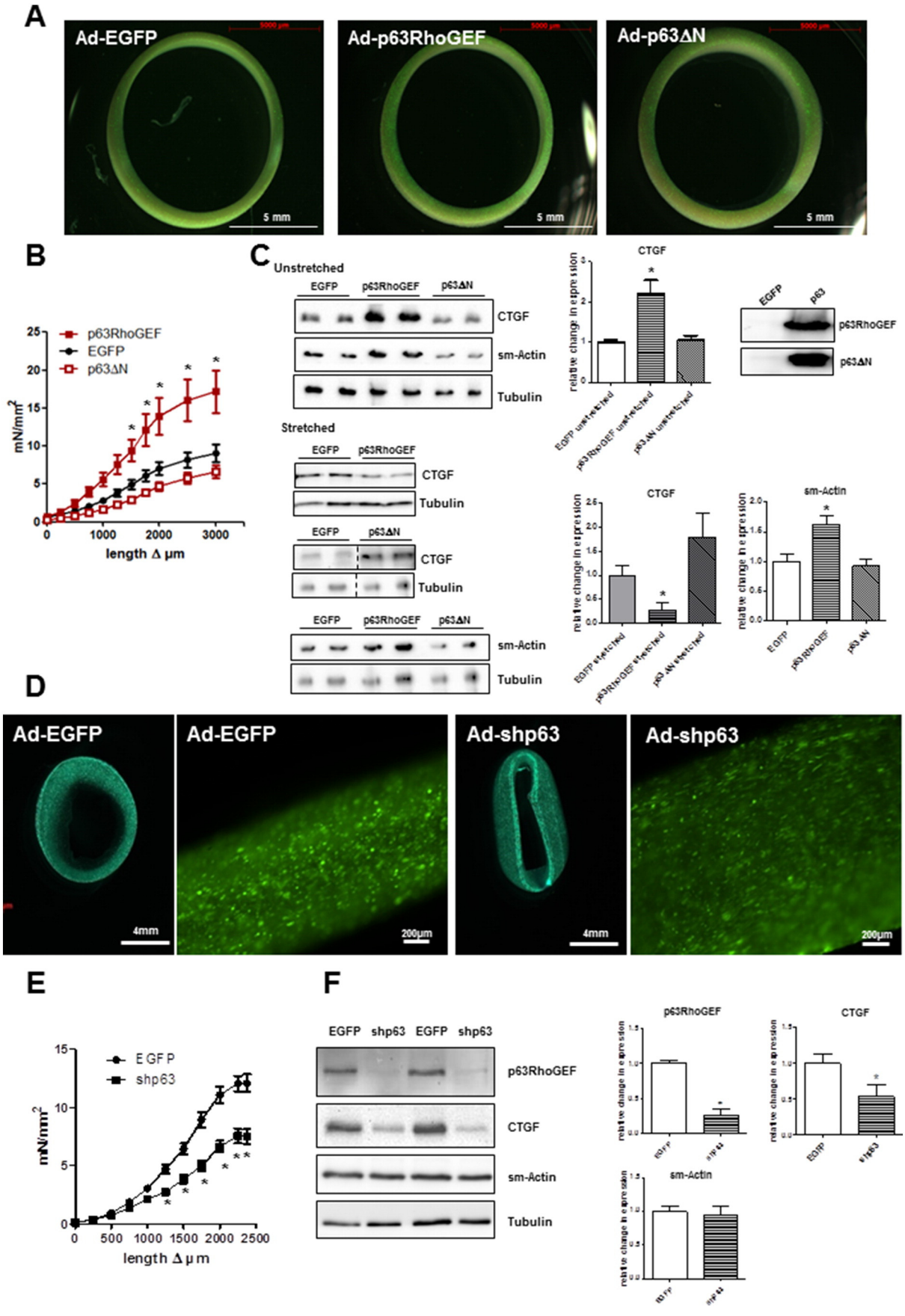
A
Ad-EGFP
Ad-p63RhoGEF
Ad-p63ΔN
5 mm
B
p63RhoGEF
EGFP
p63ΔN
mN/mm²
length Δ µm
C
Unstretched
EGFP
p63RhoGEF
p63ΔN
CTGF
sm-Actin
Tubulin
Stretched
relative change in expression
D
Ad-EGFP
Ad-shp63
4mm
200µm
E
EGFP
shp63
F
p63RhoGEF

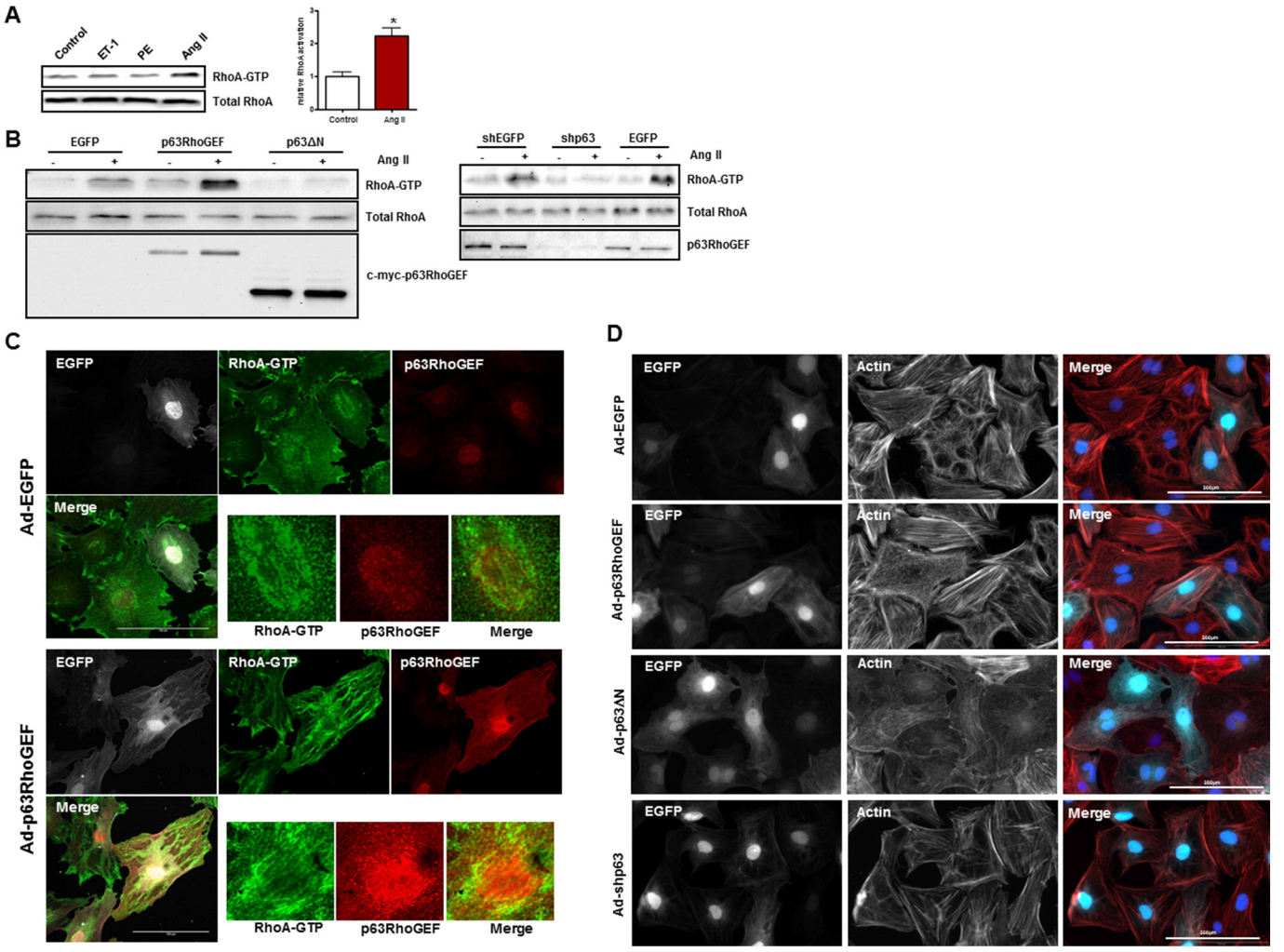

Fig. 4. p63RhoGEF mediates the Ang II-dependent RhoA activation in NRCF. A) Serum-starved NRCFs were treated with 100 nM ET-1, 10 μM PE or 100 nM Ang II for 30 s and RhoA activation was determined by pulldown assay and subsequent immunoblot analysis. Ang II-induced RhoA activation is given relative to unstimulated control as means ± SEM, n = 15, *p < 0.05. B) NRCFs were transduced for 24 h with Ad-EGFP, Ad-p63RhoGEF, Ad-p63ΔN, or for 72 h with Ad-EGFP, Ad-shEGFP, Ad-shp63 and 100 nM Ang II was added for 30 s. RhoA activation was determined by pulldown assay and subsequent immunoblot analysis. p63RhoGEF overexpression was analyzed with a c-myc antibody, p63RhoGEF downregulation was analyzed with a protein-specific antibody. Representative immunoblots are shown. Pulldown assays were repeated 2 to 3 times. C) Confocal imaging of active RhoA (RhoA-GTP) and p63RhoGEF in Ad-EGFP (upper two rows) or Ad-p63RhoGEF (lower two rows) transduced NRCF. Shown are in addition the detection of EGFP and the merge (left panels), as well as magnifications of the nuclear region (small panels). D) NRCF were transduced with Ad-p63RhoGEF and Ad-p63ΔN for 24 h, with Ad-EGFP or Ad-shp63 for 72 h and fixed. EGFP fluorescence, actin cytoskeleton staining with TRITC-phalloidin and the merge additionally containing DAPI is shown in a magnification of 200×.

night at 4 °C and washed once with cold 70% ethanol. Thereafter, the tissues were placed in 6-well plates and embedded in 2% agarose in 1 × TAE-buffer. After polymerization, the tissues were sectioned in 100 μm slices using a vibratome (Leica).

2.7. Preparation and measurement of engineered connective tissue (ECT)

NRCFs were seeded in 15 cm dishes for 2 d and transduced under serum-starved conditions with Ad-EGFP or Ad-shp63 adenoviruses (multiplicity of infection 100) for 72 h. Cells were harvested with trypsin and ECTs were prepared similarly as EHM with lower input cell number (1.5×10^6 transduced NRCF) and without Matrigel. Alternatively, NRCF, adenoviruses (Ad-EGFP, Ad-p63RhoGEF, Ad-p63ΔN) and matrix proteins were directly mixed. After polymerization, 7 ml ECT culture medium (DMEM GlutaMAX with 4,5 g/l glucose, 10% FCS, 100 U/ml penicillin, 100 μg/ml streptomycin, 1% NEAA) were added to the dish. After 4 d in culture, ECTs were subjected to similar conditions as described above for the force measurements in EHM to assess ECT stiffness by stepwise increasing the preload while measuring resting force (i.e., passive force) given normalized to the cross sectional area. For further analysis tissues before and after measurements/stretch were treated as describe above for EHM.

Fig. 5. p63RhoGEF is involved in the regulation of CTGF in NRCF. A) NRCFs were treated with 100 nM Ang II, 100 nM ET-1 or 10 μM PE for 24 h. The amounts of intracellular and secreted CTGF were determined by immunoblot analyses of cell lysates and conditioned media. CTGF values are normalized to tubulin and given as means ± SEM relative to unstimulated control, n = 6–7,*p < 0.05. Representative immunoblots are shown. B) NRCFs were treated with 100 nM Ang II for 24 h. Amount of intracellular and secreted CTGF was determined. Total CTGF is set to 100%. Relative distribution in cell lysates and conditioned media is shown. Values are means ± SEM; n = 6. C) CTGF was detected by indirect immunofluorescence. DAPI and WGA were used as co-staining. The merge is also shown (magnification 400×). D–F) NRCFs were transduced with Ad-EGFP, Ad-p63RhoGEF or Ad-p63ΔN for 24 h or Ad-EGFP or Ad-shp63 for 72 h and stimulated with 100 nM Ang II for 24 h. The amounts of intracellular and secreted CTGF were determined by immunoblots of cell lysates and conditioned media. In addition, p63RhoGEF expression was analyzed. Representative immunoblots are shown. Values are given as means ± SEM, normalized to tubulin and relative to EGFP, *p < 0.05 vs. EGFP, #p < 0.05 vs. EGFP + Ang II, n = 5–12.

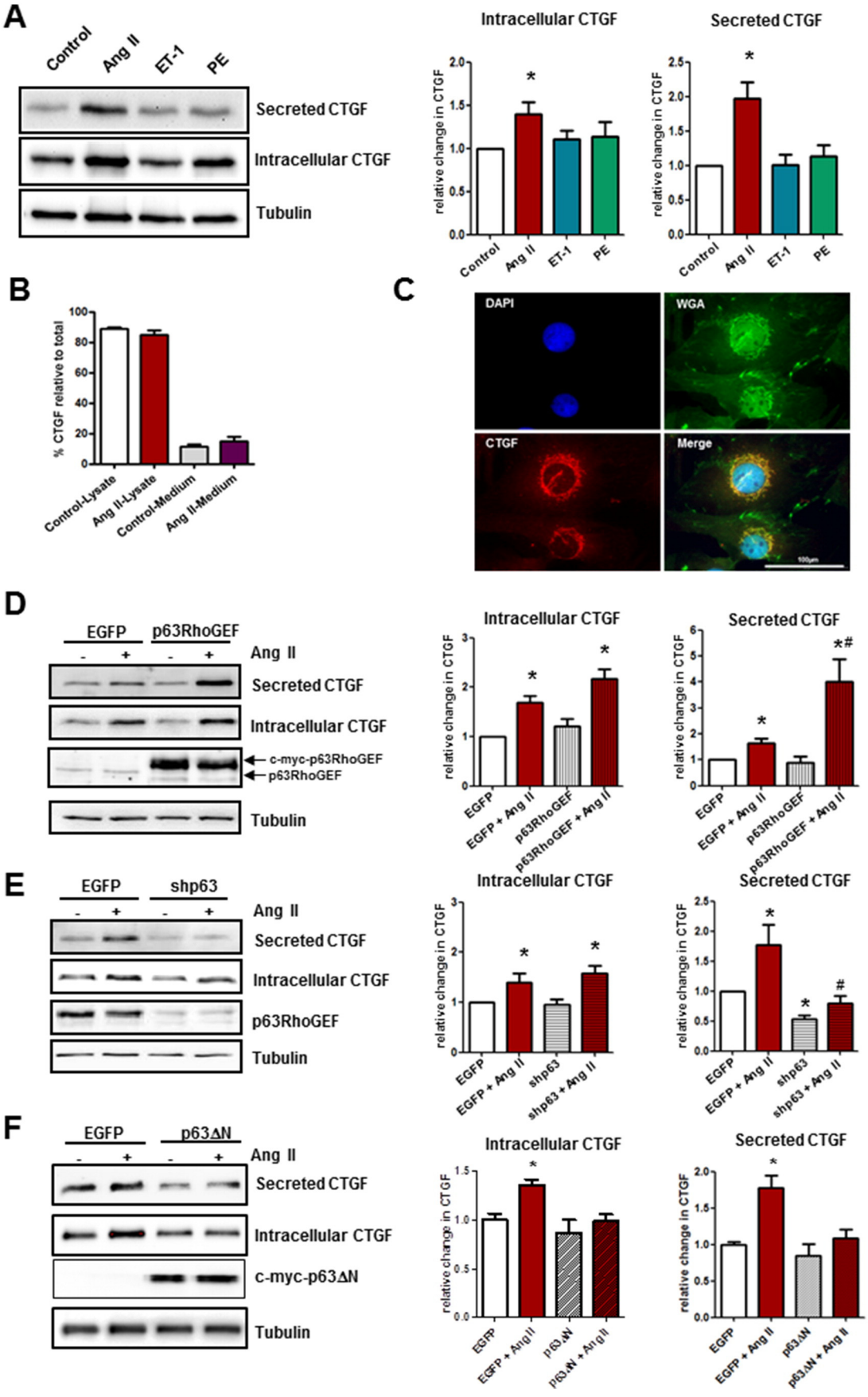
A
Control
Ang II
ET-1
PE
Secreted CTGF
Intracellular CTGF
Tubulin
Intracellular CTGF
Secreted CTGF
relative change in CTGF
B
% CTGF relative to total
Control-Lysate
Ang II-Lysate
Control-Medium
Ang II-Medium
C
DAPI
WGA
CTGF
Merge
D
EGFP
p63RhoGEF
Ang II
Secreted CTGF
Intracellular CTGF
c-myc-p63RhoGEF
p63RhoGEF
Tubulin
EGFP + Ang II
p63RhoGEF + Ang II
E
shp63
p63RhoGEF
shp63 + Ang II
F
p63ΔN
c-myc-p63ΔN
p63ΔN + Ang II

2.8. RhoA activation assay

RhoA activation was measured by pulldown experiments using the Rho-binding domain of rhotekin as described previously [31]. In brief, P1 NRCFs were cultured in 10 cm dishes, then adenovirally transduced under serum-starved conditions for 24 h or for 72 h in cases of the knockdown experiment. Alternatively, NRCFs were serum-starved for 24 h prior to the assay. Activation of RhoA was induced with 100 nM Ang II, 100 nM ET-1 or 10 μM PE for 30 s as indicated. Cell lysis was carried out on ice with ice-cold GST-Fish buffer. Cells were scraped off, the homogenates were cleared by centrifugation at 15,000 *g* and 4 °C for 10 min. Then the lysate was incubated with 40 μg of the Rho-binding domain of rhotekin fused to GST and coupled to Glutathione Sepharose (GE Healthcare) for 1 h. The bound protein was precipitated, washed twice with GST-Fish buffer and subjected to immunoblot analysis. In addition, a fraction of the total cell lysate was analyzed.

2.9. Measurement of intracellular and secreted CTGF

P1 NRCFs were cultured in 12-well plates, serum-starved for 24 h and stimulated with 100 nM Ang II, 100 nM ET-1 or 10 μM PE for 24 h. To analyze the effect of p63RhoGEF, P1 NRCFs were cultured in 12-well plates, then adenovirally transduced under serum-starved conditions with Ad-EGFP, Ad-p63RhoGEF and Ad-p63ΔN for 24 h or Ad-EGFP and Ad-shp63 for 72 h and treated then with 100 nM Ang II for 24 h. In other cases, P1 NRCFs were cultured in 12-well plates, serum-starved for 24 h, pre-incubated with fasudil (10 μM), H1152p (300 nM), C3T (Cytoskeleton, 1 μg/ml), CCG1423 (10 μM) or LatA (5.5, 7.0 or 8.5 ng/ml) for 1 h and then treated with 100 nM Ang II for 24 h. In all cases conditioned media were taken for analysis of secreted CTGF and cells were lysed in GST-Fish buffer as described above. The amount of secreted and intracellular CTGF was analyzed by immunoblot.

2.10. Assay of SRF activation

NRCFs were seeded onto 12-well plates and co-transfected with 1.37 μg pSRE.L-luciferase reporter plasmid [32] and 0.23 μg pRL.TK control reporter vector with Lipofectamine 2000 (Invitrogen) according to the manufacturer's protocol. Alternatively, NRCFs were transfected in 24-well plates with 0.5 μg empty pCMV-Tag3, pCMV-Tag3-p63RhoGEF or pCMV-Tag3-p63ΔN plus 0.4 μg pSRE.L and 0.1 μg pRL.TK with Lipofectamine 3000 (Invitrogen). Twenty-four to 48 h after transfection, cells were washed once with PBS, serum-starved for 24 h, pre-incubated with 10 μM fasudil, 300 nM H1152p, 1 μg/ml C3T or 10 μM CCG1423 for 30 min, and treated with 100 nM Ang II for 24 h. Luciferase activities were determined with the Dual-Luciferase reporter assay system (Promega) as described before [31] and measured with a Multilabel Reader EnVision (Perkin Elmer). The firefly luciferase activities were normalized to the respective renilla luciferase activities. Ratios of untreated controls were set to 1.

2.11. Immunoblot analysis

Protein samples, resulting from 2D or 3D (EHM/ECT) cell culture models or homogenated heart tissue in GST-Fish buffer, were separated in 8% to 15% SDS-PAGE and subsequently transferred onto nitrocellulose membranes. After blocking with Roti-block (Carl Roth) for 1 h, the membranes were incubated with the following antibodies overnight at 4 °C: anti-β-actin (1:2000), anti-smooth muscle-actin (1:2000), anti-vimentin (1:2000) and anti-tubulin (1:2000) from Sigma-Aldrich, anti-p63RhoGEF (1:1000) from Proteintech Group, anti-GAPDH (1:50,000) from Zytomed, anti-CTGF (1:200), anti-RhoA (1:200), anti-c-Myc and anti-Rock1 (1:200) from Santa Cruz. After incubation with appropriate secondary antibodies for 1 h, proteins were visualized by enhanced chemoluminescence (Lumi-Light^{Plus} Western blotting Substrate, Roche) in a VersaDoc-Imaging System (Bio-Rad Laboratories). For quantification of the immunoblots Quantity One 1-D Analysis Software (Bio-Rad Laboratories) was used.

2.12. Immunofluorescence staining and microscope image acquisition

For microscopy, differently treated cells seeded on 12-well dishes or on collagen-coated coverslips were fixed in 4% formaldehyde in PBS for 15 min, permeabilized in 0.05% Triton-X 100 in PBS for 3 min and blocked for 1 h with Roti-Block (Roth). In addition, vibratome sections were used, which were blocked/permeabilized in 1% BSA, 0.5% Triton X-100 in PBS over night at 4 °C. Independent of the sample, incubation with primary antibodies against p63RhoGEF (Proteintech Group), Rho-GTP (NewEast Biosciences) CTGF (Santa Cruz), KDEL (Abcam), GOPC (Sigma), Lamp2 (Sigma), Gm130 (Becton Dickinson) was performed in PBS over night at 4 °C, incubation with fluorochrome-labeled secondary antibodies (Jackson ImmunoResearch), DAPI, TRITC- or FITC-labeled phalloidin or Alexa Fluor® 488-labeled WGA were performed in PBS for 1 h at room temperature. Samples were stored in PBS at 4 °C and imaged on an inverted microscope (Olympus) with a XM 10 T camera (Olympus) using 4×–60× objectives at room temperature. Cell^{M} Software (Olympus) was used for image processing including adjustments of brightness and contrast. In addition, cells and sections were analyzed by confocal microscopy by using a confocal laser scanning microscope LSM 710 (Zeiss) with 20 × 0.5 NA and 63 × 1.4 NA oil objectives. Images were recorded with the Zen 2009 software.

2.13. mRNA isolation, reverse transcription and quantitative PCR

Total RNA was isolated from heart tissue using the TissueLyser and RNeasy mini Kit (Qiagen) or from NRCF using QiaShredder columns. cDNA was synthesized by reverse transcription using the RevertAid First Strand cDNA Synthesis Kit (Thermo Scientific) according to the manufacturer's instructions. Quantitative real-time PCR was performed using the Hot FirePol Eva Green Polymerase (Solis BioDyne) or the QuantiFast SYBR Green PCR Kit (Qiagen) and an Abi7900HT instrument (Applied Biosystems). Relative cDNA amounts were calculated by SDS 2.4 software with help of a standard curve performed for each primer pair using a pool of all cDNAs. All reactions were run in triplicates and normalized to porphobilinogen deaminase (PBGD). Following primer sets were used:

PBGD	for: CCTGAAACTCTGCTTCGCTG
	rev: CTGGACCATCTTCTTGCTGAA
CTGF	for: CCGGGTTACCAATGACAATA
	rev: CACACCCCACAGAACTTAGC
Pro-Col1a1	for: TTCACCTACAGCACGCTTGT
	rev: TTGGGATGGAGGGAGTTTAC
TGF-β1	for: AGAGCCCTGGATACCAACTA
	rev: TGTTGGTTGTAGAGGGCAAG
Biglycan	for: CTGAGGGAACTTCACTTGGA
	rev: CAGATAGACAACCTGGAGGA
sm-Actin	for: CATCAGGAACCTCGAGAAGC
	rev: TCGGATACTTCAGGGTCAGG

2.14. Statistics

Results are presented as means ± SEM. Data were analyzed by 1way or 2way ANOVA, followed by Bonferroni's Multiple Comparison Test as

Fig. 6. p63RhoGEF regulates the gene transcription of fibroblast genes. NRCF were transduced with Ad-EGFP or Ad-p63RhoGEF for 24 h, with Ad-EGFP or Ad-shp63 for 72 h and treated with 100 nM Ang II. Total RNA isolation, cDNA synthesis and qPCR were performed. Values are normalized to PBGD and relative to EGFP and given as means ± SEM, n > 4, *p < 0.05 vs. EGFP or as indicated by the line. A) CTGF qPCR after 2 h (left graph) and 24 h (right graph) of Ang II treatment B) TGF-β1 qPCR after 2 h of Ang II treatment C–E) sm-actin, biglycan and collagen1α1 qPCR after 24 h of Ang II treatment.

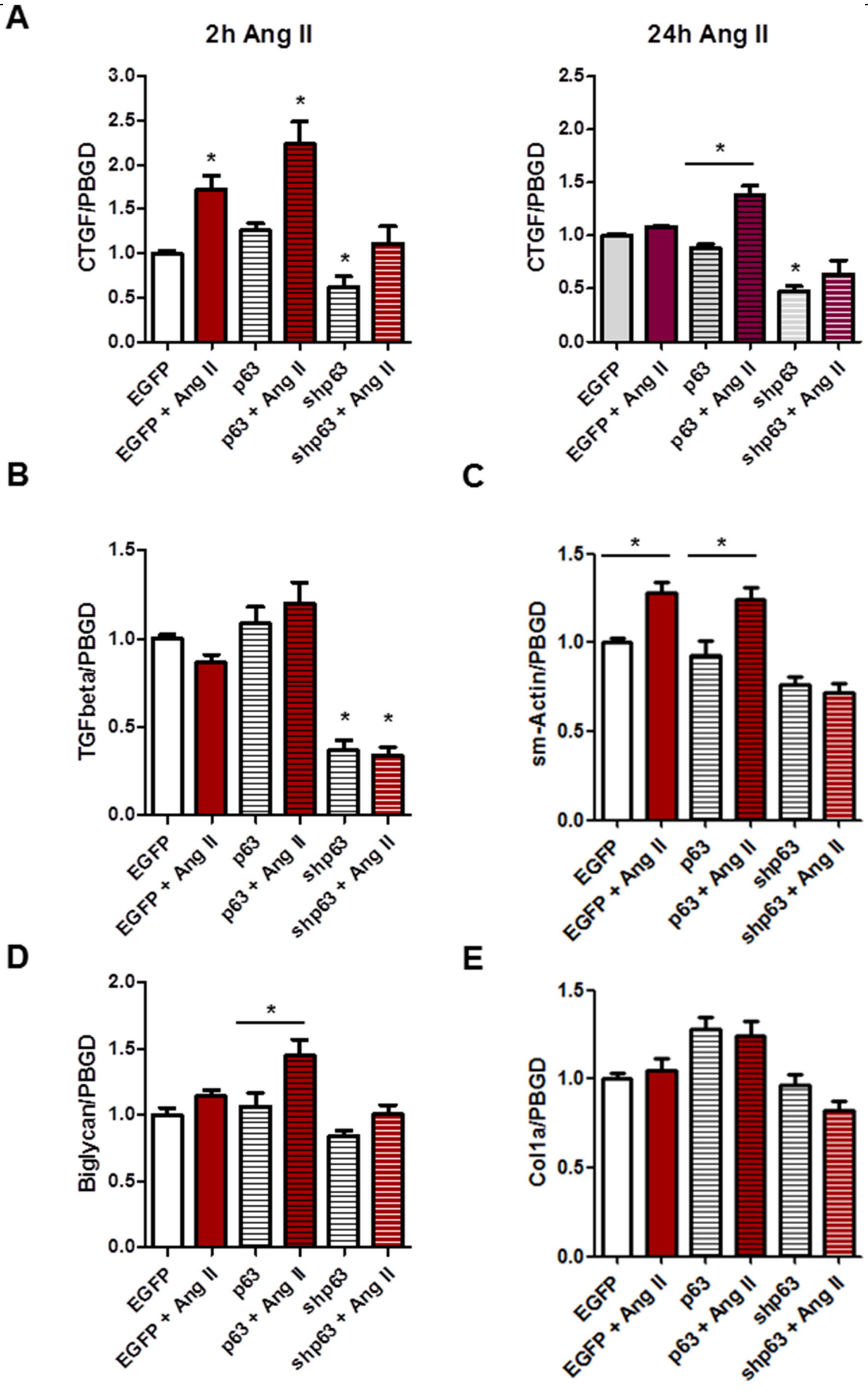
A
2h Ang II
24h Ang II
CTGF/PBGD
B
TGFbeta/PBGD
C
sm-Actin/PBGD
D
Biglycan/PBGD
E
Col1a/PBGD
EGFP
EGFP + Ang II
p63
p63 + Ang II
shp63
shp63 + Ang II

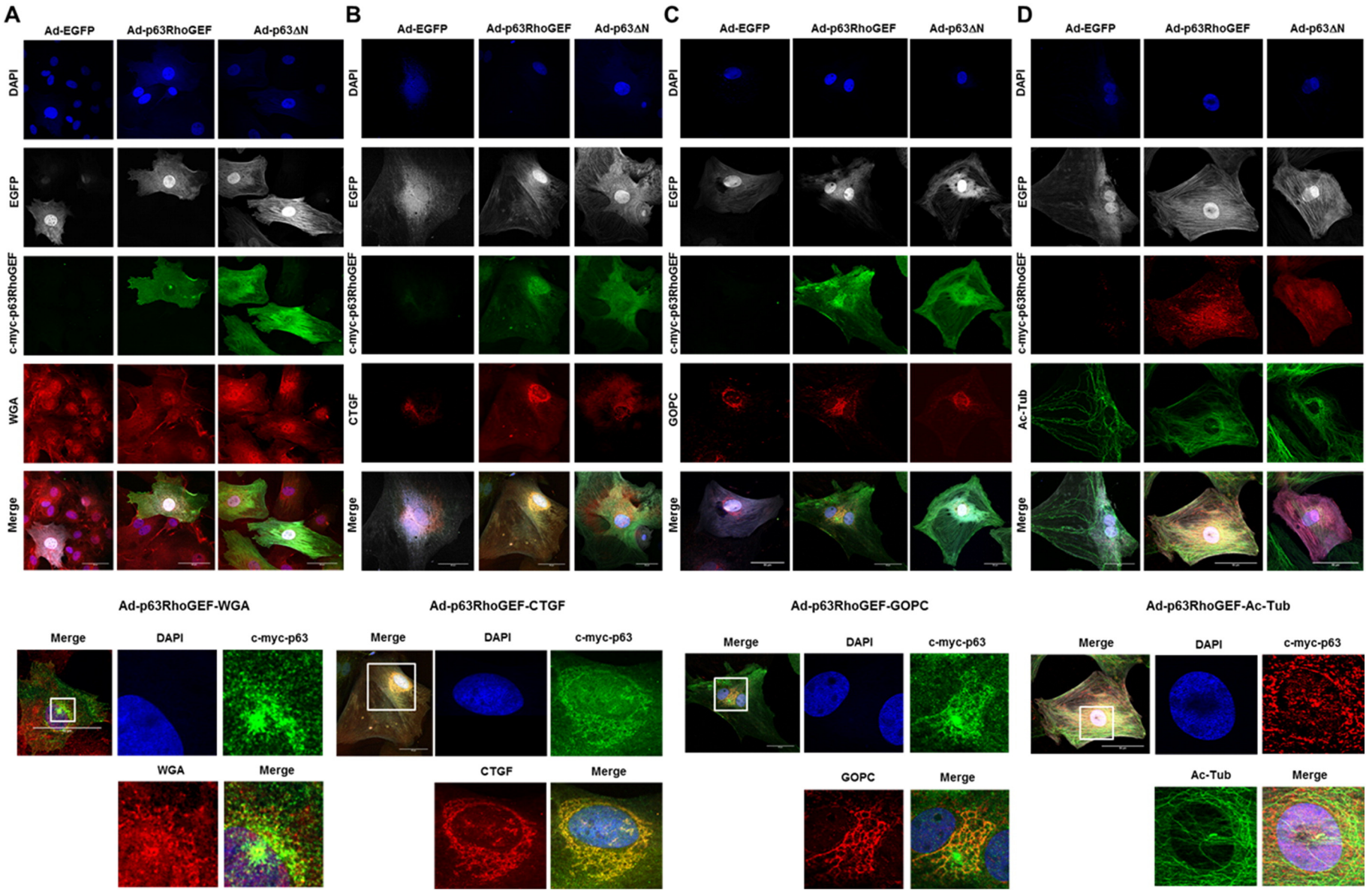

Fig. 7. p63RhoGEF localizes at intracellular membrane structures involved in secretion. NRCFs were transduced with Ad-EGFP, Ad-p63RhoGEF or Ad-p63ΔN for 24 h, fixed and confocal imaging was performed. Nuclei were stained with DAPI. Adenoviral transduction was detected by EGFP. p63RhoGEF and p63ΔN were detected with a c-myc antibody. In addition, WGA was used to stain glycosylated membrane proteins (A). CTGF (B), the trans-Golgi network GOPC (C) and acetylated tubulin (D) were detected with specific antibodies. In the last row the merges are shown and underneath higher magnifications of the Ad-p63RhoGEF transduced NRCF.

well as by unpaired t-test. p values of less than 0.05 were considered statistically significant.

3. Results

3.1. p63RhoGEF and CTGF are up-regulated by an increase in cardiac afterload

To elucidate the role of p63RhoGEF in the heart and its potential function in the regulation of CTGF, we performed a pilot expression study with heart tissue from mice which were subjected to transverse aortic constriction (TAC) or sham surgery. After 1 week, when the left ventricular weight/tibia length was increased by 22% and fibrosis could be already detected, without an impairment of the contractile function (for detailed information: [25]), the expression of p63RhoGEF and CTGF was significantly increased by 2- and 6.6-folds, respectively. This was independent from the chosen normalization marker (Fig. 1A). To further validate this finding in a second series, TAC-operated mice were allowed to acquire a more severe phenotype, including a mean 70% increase in the left ventricular weight to body weight ratio (LVW/BW), a decrease in the ejection fraction (EF) from 41% to 29% and an increase in the systolic and diastolic volume (Vs and Vd) of the left ventricle by 62% and 31%, respectively (Suppl. Fig. S1). By qPCR we could show that, compared to sham-operated mice, the mean expression of p63RhoGEF and CTGF were increased by 1.5- and 3.3-folds (Fig. 1B), respectively. More importantly, independent from sex, the p63RhoGEF expression positively correlates with CTGF (Fig. 1B), Vd, Vs (Fig. 1C) and the LVW/BW (Suppl. Fig. S1) as well as negatively correlates with the EF (Fig. 1C).

3.2. p63RhoGEF in cardiac fibroblasts regulates contractility of engineered heart muscle tissues

In previously published data on p63RhoGEF [22], we were able to show that this activator of RhoA is more strongly expressed in cardiac fibroblasts than in cardiomyocytes (see also Suppl. Fig. S2). Therefore, we analyzed whether the up-regulation of p63RhoGEF in neonatal rat cardiac fibroblasts (NRCFs) in engineered heart muscle (EHM) is sufficient to induce CTGF expression in the absence of the neurohumoral stimulation occurring as a consequence of the afterload increase in mice. For this, we adenovirally transduced NRCF and supplemented these cells with total cardiac cells in a 1:5 ratio for EHM preparation. The predominant transduction of NRCF and their equal distribution in the tissue was ensured based on the viral marker EGFP (Fig. 2A, upper panels, left: Ad-EGFP transduced, right: Ad-p63RhoGEF transduced) as well as by α-actinin/EGFP detection via confocal microscopy (Fig. 2A, lower panels, left: Ad-EGFP transduced, right: Ad-p63RhoGEF transduced). By immunoblot, the overexpression of p63RhoGEF was verified and CTGF expression was demonstrated to be 2-fold up-regulated in these EHMs. For control, the comparable content of cardiomyocytes and cardiac (myo)fibroblasts was shown by their marker calsequestrin-2 (CSQ) and sm-actin, respectively (Fig. 2B). The measured resting and twitch tensions of EHM containing p63RhoGEF-expressing NRCF were interestingly significantly increased independent of the present calcium concentration (Fig. 2C, left and right panel). In contrast, when the adenoviral transduction was performed after EHM condensation no changes could be observed. This procedure mainly resulted in a transduction of the more prone cardiomyocytes as detected by confocal imaging (Suppl. Fig. S3A–C). To further validate the importance of p63RhoGEF in cardiac fibroblasts, we overexpressed in NRCF a dominant negative p63RhoGEF construct (p63ΔN) which blocks the $G_{q/11}$-dependent RhoA activation [20] and prepared again extra-fibroblast-containing EHM (Fig. 2D). This resulted in a lower expression of CTGF and a reduced resting and twitch tension by trend (Fig. 2E, F). This data suggests that p63RhoGEF in cardiac fibroblasts regulates paracrine signaling and thus contractile function of heart muscle tissues.

3.3. p63RhoGEF regulates the stiffness of engineered connective tissues

We further investigated the impact of p63RhoGEF on the viscoelastic properties of engineered cardiac connective tissue mainly composed of adenovirally transduced NRCF and collagen. Equal distribution and transduction of fibroblasts were assessed by imaging of the co-expressed EGFP (Fig. 3A, D). Up-regulation of p63RhoGEF in NRCF resulted in a significant increased stiffness of ECT whereas p63ΔN reduced stiffness by trend (Fig. 3B). Analysis of CTGF expression demonstrated that before stretch its content is higher in p63RhoGEF-expressing ECT whereas after stretch it was significantly lower compared to control ECT. In addition, sm-actin was increased in p63RhoGEF-expressing ECT independent of stretch. In p63ΔN-expressing ECT no significant changes could be observed (Fig. 3C). In contrast, ECT composed of NRCF with a knockdown of p63RhoGEF (shp63) displayed a strongly reduced stiffness (Fig. 3E) accompanied by a reduced expression of CTGF. Sm-actin was not changed in these ECTs (Fig. 3F).

3.4. p63RhoGEF mediates Ang II-induced RhoA activation in cardiac fibroblasts

To further establish the role of p63RhoGEF in the regulation of auto- and paracrine signaling in cardiac fibroblasts, we performed several experiments with purified 2D cultures of NRCF. This allows the use of specific stimuli and thus a detailed analysis of the underlying signaling. First, we treated the cells with the GPCR agonists Ang II, ET-1 or phenylephrine (PE) and identified Ang II as the only efficient activator of RhoA (Fig. 4A). Next, we studied the impact of p63RhoGEF overexpression and knockdown as well as of p63ΔN on the RhoA activity and could show that the latter two blunted the Ang II-dependent RhoA activation whereas the full length protein increased the basal as well as the Ang II-dependent activity (Fig. 4B). By confocal microscopy using specific antibodies against GTP-bound RhoA and p63RhoGEF the impact of p63RhoGEF on the basal RhoA activation could be confirmed (Fig. 4C). To exclude transduction artifacts two types of control adenoviruses were included in these experiments (EGFP and shEGFP). Moreover, we overexpressed the RGS-domain of the murine p115-RhoGEF homolog Lsc to inhibit $G_{12/13}$ proteins [33], but found no effect on the Ang II-dependent RhoA activation (Suppl. Fig. S4).

As the RhoA activity is pivotal for the regulation of the actin cytoskeleton, we stained transduced NRCF with fluorophore-labeled phalloidin and found that p63RhoGEF expression had no obvious additional effect on the already in control transduced cells existing extensive actin structures. The knockdown and p63ΔN expression, however, reduced the complexity of the actin cytoskeleton (Fig. 4D). From these experiments we conclude that p63RhoGEF is an important mediator of the Ang II-induced RhoA activation in NRCF and influences the actin cytoskeleton.

3.5. p63RhoGEF regulates CTGF in NRCF in response to Ang II

Next we analyzed the GPCR-dependent regulation of CTGF in NRCF. Therefore, the cells were treated with Ang II, PE and ET-1 for 24 h. This led only in case of Ang II to an increase in the intracellular and extracellular content of CTGF (Fig. 5A). We could further show that the majority of CTGF is stored intracellular in the Golgi apparatus and Ang II increased the amount of secreted CTGF from 11% to 15% (Fig. 5B, C). Next, we studied the effect of p63RhoGEF on intracellular and extracellular CTGF under basal conditions and after Ang II treatment. Our data suggest that p63RhoGEF impacts the Ang II-dependent secretion of CTGF as an increase or decrease of this GEF resulted in paralleled changes in extracellular CTGF. The intracellular amounts were not altered (Fig. 5D, E). However, the $G_{q/11}$ inhibitor p63ΔN was sufficient to

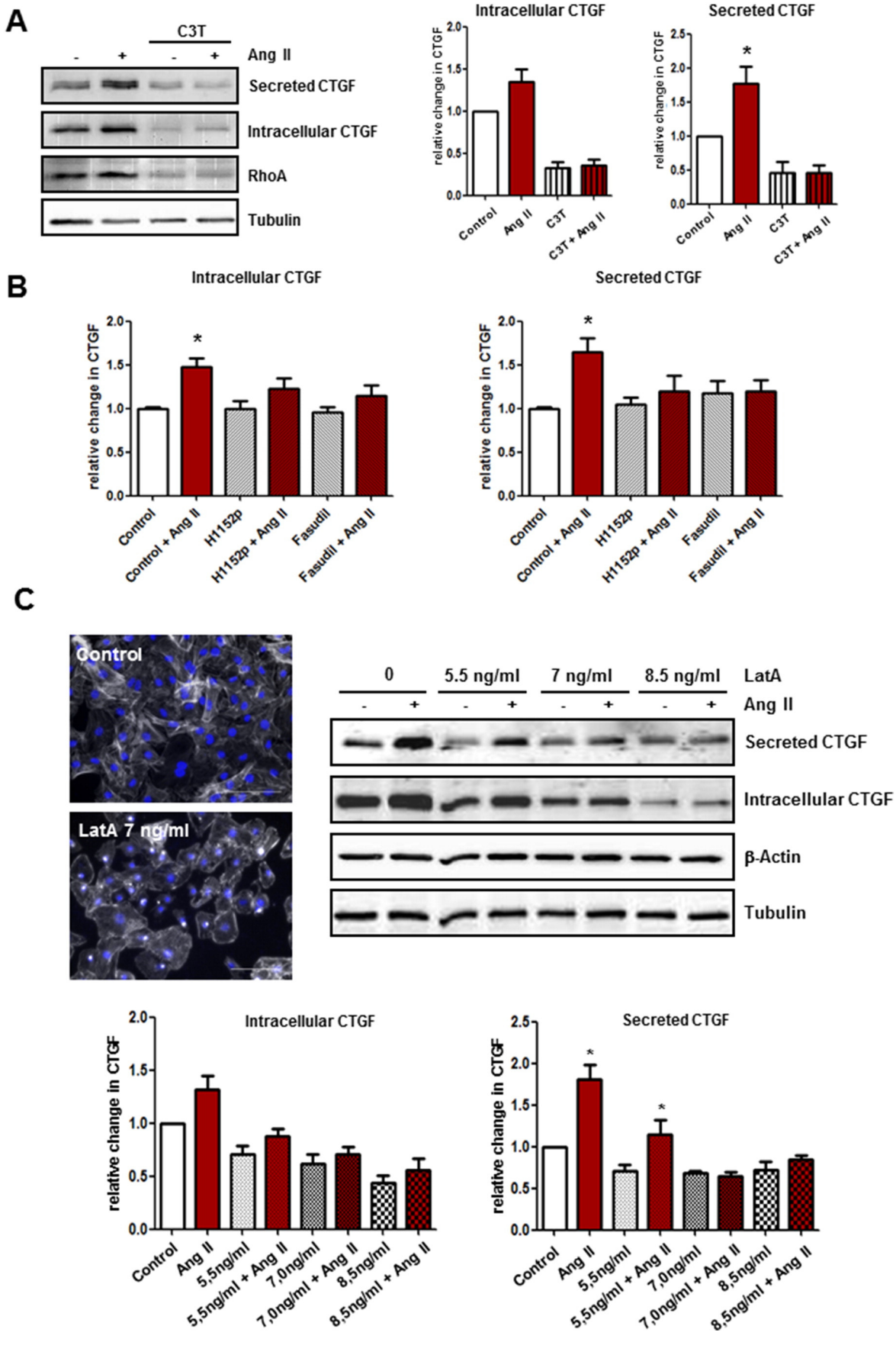
A
C3T
- + - +
Ang II
Secreted CTGF
Intracellular CTGF
RhoA
Tubulin
Intracellular CTGF
relative change in CTGF
Control
Ang II
C3T
C3T + Ang II
Secreted CTGF
B
Intracellular CTGF
Secreted CTGF
Control
Control + Ang II
H1152p
H1152p + Ang II
Fasudil
Fasudil + Ang II
C
Control
LatA 7 ng/ml
0
5.5 ng/ml
7 ng/ml
8.5 ng/ml
LatA
Ang II
Secreted CTGF
Intracellular CTGF
β-Actin
Tubulin
Intracellular CTGF
Secreted CTGF
Control
Ang II
5,5ng/ml
5,5ng/ml + Ang II
7,0ng/ml
7,0ng/ml + Ang II
8,5ng/ml
8,5ng/ml + Ang II

block the intracellular and extracellular increase of CTGF arguing for an additional involvement of other $G_{q/11}$-mediated signal pathways (Fig. 5F).

3.6. p63RhoGEF regulates the expression of typical cardiac (myo)fibroblast genes

Although p63RhoGEF did not influence the intracellular amounts of CTGF, a change in expression, reflecting the sum of intra- and extracellular CTGF, can be assumed. Therefore, we performed qPCR studies in which we found CTGF to be rapidly and transiently induced by Ang II within 2 h and returned to basal level after 24 h in control transduced NRCF. In cells overexpressing p63RhoGEF the response after 2 h of stimulation was not different from control cells, however, after 24 h a significant increase was still detectable. The knockdown of p63RhoGEF led after 2 h and 24 h to a reduction in basal CTGF transcription and also the Ang II-mediated effect was reduced after 2 h (Fig. 6A). We further analyzed the transcription of TGF-β1 after 2 h as a supposed link between Ang II and the immediate early CTGF expression, but could not detect a significant induction. p63RhoGEF overexpression was also without effect. Interestingly, in p63RhoGEF-knockdown cells TGF-β1 gene transcription was significantly lower than in control cells (Fig. 6B). All other genes, which are regulated with a slower time course, were studied after 24 h treatment with Ang II. For smooth muscle-actin a small increase in gene expression was found in control and p63RhoGEF-overexpressing cells, but not in knockdown cells (Fig. 6C). In contrast to other publications [34,35], we found no impact of Ang II on the transcription of pro-collagen 1α1 and on the collagen organizing proteoglycan biglycan. Only after p63RhoGEF overexpression and Ang II treatment an increase of biglycan could be detected, but still not for collagen (Fig. 6D, E).

3.7. p63RhoGEF localizes at intracellular membrane structures involved in secretion

To further analyze the role of p63RhoGEF in NRCF and especially in the regulation of protein secretion, we performed confocal analysis studies. As in Fig. 4C a perinuclear/nuclear staining of p63RhoGEF was apparent, we first compared its localization pattern by using different antibodies, including a p63RhoGEF-specific and two c-myc-tag specific antibodies, recognizing overexpressed c-myc-tagged p63RhoGEF in cardiac fibroblasts transduced with either Ad-EGFP, Ad-p63RhoGEF or Ad-p63ΔN (Suppl. Fig. S5A). In addition, co-staining of the p63RhoGEF and c-myc-tag antibodies were performed with subsequent z-stack analysis (Suppl. Fig. S5B) arguing for a predominant localization of full length p63RhoGEF associated with intracellular membrane compartments. The strong nuclear signal detected by the p63RhoGEF antibody is most likely unspecific as this was not comparably detected by the c-myc-antibodies. However, we could not fully rule out that a small portion of p63RhoGEF might be located in the nucleus. Further studies on the localization of p63RhoGEF revealed that it can be detected in vicinity to WGA-positive membranes, closely associated with CTGF and to the trans-Golgi apparatus network (Fig. 7A–C), but not to the endoplasmic reticulum membranes, lysosomes and the cis-Golgi apparatus network (Suppl. Fig. S6A–C). Interestingly, in many cells expressing p63RhoGEF a distinct punctual localization at or close to the nucleus was detected which was located at the base of primary cilia as shown by co-staining of acetylated tubulin, the main structural component of these cellular organelles (Fig. 7D). In contrast to full length p63RhoGEF, p63ΔN was located mainly in the cytosol (Suppl. Figs. S5A, 7A–D) and in some cells in the nucleus (e.g. Suppl. Figs. S5A, S6B, C), which might explain some of its divergent actions like the inhibition of intracellular CTGF.

3.8. The induction of CTGF expression and secretion is dependent on RhoA/ROCK activity and on the integrity of the actin cytoskeleton

In order to verify the involvement of RhoA in the regulation of CTGF in NRCF, we treated the cells with a cell-permeant variant of the RhoA/B/C-inhibitor C3 transferase (C3T) from *Clostridium botulinum*. C3T treatment led to reduction of basal as well as Ang II-induced CTGF expression and secretion (Fig. 8A). Moreover, we used the two Rho-associated kinase (ROCK) inhibitors fasudil, which additionally inhibits protein kinase N, and the more potent H1152p and could show that both inhibitors were able to reduce the Ang II-induced expression and secretion of CTGF in NRCF (Fig. 8B). To validate the involvement of the actin cytoskeleton, we treated the NRCF with latrunculin A (LatA), an actin filament disrupting toxin, and found a concentration-dependent inhibition of CTGF expression and secretion and the expected disintegration of the actin cytoskeleton (Fig. 8C).

3.9. The p63RhoGEF-dependent regulation of CTGF involves the serum response factor

Based on the recent literature [18,36] we hypothesized that the serum response factor (SRF) is involved in the p63RhoGEF-dependent regulation of CTGF. The activation of the SRF was determined by luciferase reporter gene assays in NRCF. In control transfected cells, Ang II increased the SRF activity by 1.5-fold. In NRCF expressing p63ΔN no increase in response to Ang II was detected, and in p63RhoGEF expressing cells the increase was approx. 4-fold (Fig. 9A). Moreover, RhoA inhibition by C3T blunted the Ang II effect similar to p63ΔN (Fig. 9B). ROCK inhibition by H1152p was not sufficient to inhibit the Ang II effect, but fasudil was (Fig. 9C). This is likely due to their different potencies in the regulation of the actin cytoskeleton as at the chosen concentration H1152p was not sufficient to interfere with the organization of actin filaments (Fig. 9D). To validate the role of the SRF in CTGF regulation, we used the myocardin-related transcription factor (MRTF) inhibitor CCG1423. MRTF is a co-factor of the SRF and thought to be an important mediator of the Rho-dependent regulation of SRF [37]. In accordance, CCG1423 treatment resulted in an inhibition of the Ang II-induced increase in SRF activity (Fig. 9E), in a disassembly of the actin cytoskeleton (Fig. 9F) and an inhibition of CTGF expression and secretion (Fig. 9G).

4. Discussion

The guanine nucleotide exchange factor p63RhoGEF was described as a specific activator of RhoA with strong expression in the heart [19]. We confirmed this finding and found that p63RhoGEF is most abundantly expressed in smooth muscle cells as well as in cardiac fibroblasts and to a lesser extent in cardiomyocytes [22]. However, the mechanistic role of p63RhoGEF in the heart remained elusive. Here we present data arguing for a role of p63RhoGEF as a specific regulator of auto- and paracrine factors like CTGF in cardiac fibroblasts in response to classical fibrotic/remodeling stimuli such as Ang II.

Fig. 8. Rho, ROCK and actin regulates CTGF in NRCF. A, B) NRCF were pre-incubated with 1 μg/ml C3T (A) or with 10 μM fasudil or 300 nM H1152p (B) for 1 h and treated with 100 nM Ang II for 24 h. The amounts of intracellular and secreted CTGF were determined by immunoblot analyses of cell lysates and conditioned media. For C3T representative immunoblots are shown. All values are given as means ± SEM, normalized to tubulin and relative to control, *$p < 0.05$ vs. control, $n = 4–9$ for C3T (A) and $n = 20–30$ for ROCK inhibitors (B). C) NRCFs were treated with the indicated concentrations of latrunculin A (LatA) for 24 h. The actin cytoskeleton was stained with FITC-phalloidin and nuclei with DAPI, magnification 100× (upper left panel). The cells were in addition after 1 h of LatA application treated with 100 nM Ang II and intracellular and extracellular contents of CTGF were determined by immunoblot analysis. Representative blots of CTGF, tubulin and β-actin are shown (upper right panel). Quantifications of intracellular and extracellular CTGF normalized to tubulin and relative to untreated controls are given in the lower left and lower right panel, respectively. The given concentrations refer to LatA. Shown are the means ± SEM, $n = 5$, *$p < 0.05$ vs. control.

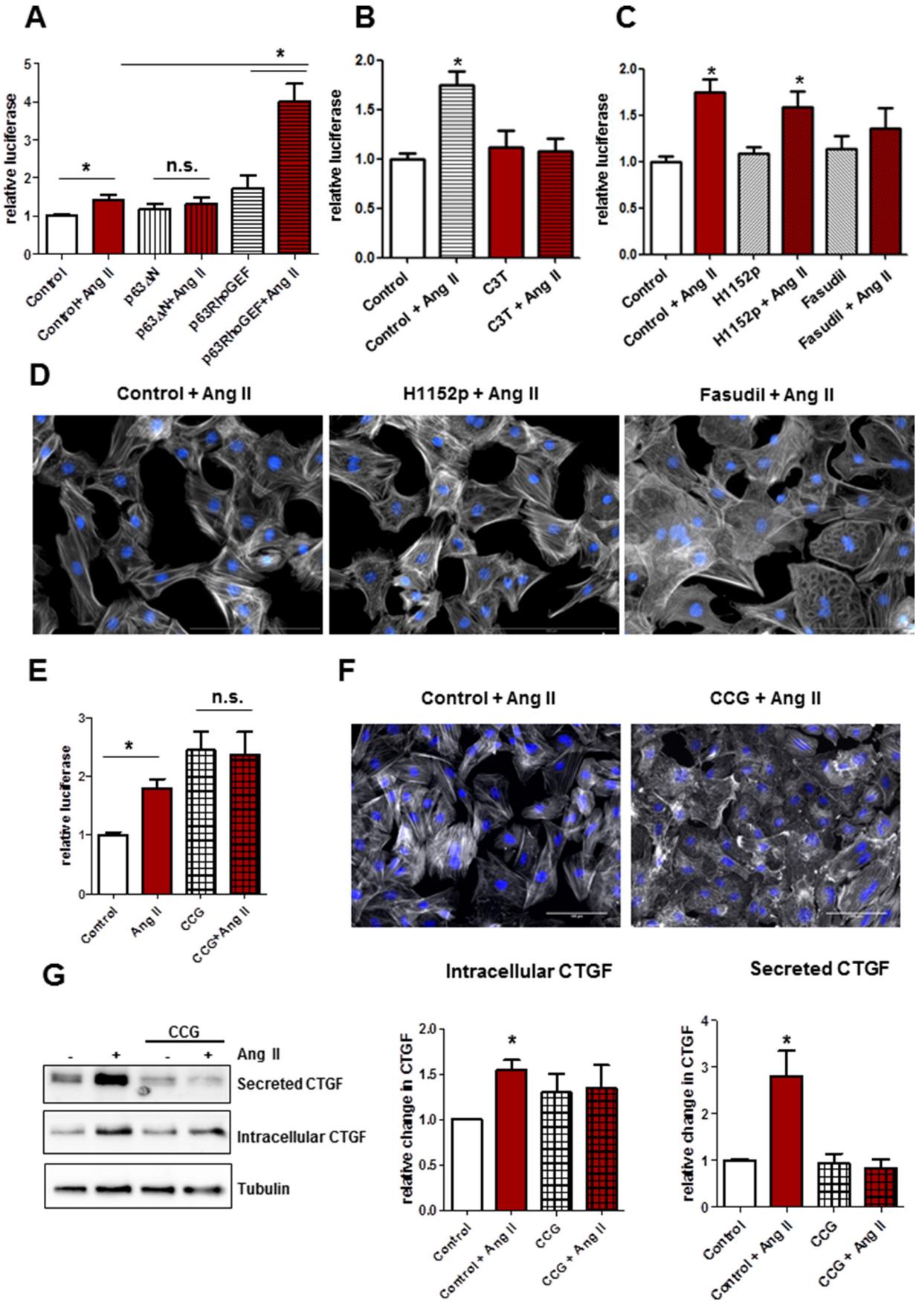
A
relative luciferase
Control
Control+Ang II
p63ΔN
p63ΔN+Ang II
p63RhoGEF
p63RhoGEF+Ang II
n.s.
B
relative luciferase
Control
Control + Ang II
C3T
C3T + Ang II
C
relative luciferase
Control
Control + Ang II
H1152p
H1152p + Ang II
Fasudil
Fasudil + Ang II
D
Control + Ang II
H1152p + Ang II
Fasudil + Ang II
E
relative luciferase
n.s.
Control
Ang II
CCG
CCG+Ang II
F
Control + Ang II
CCG + Ang II
G
CCG
Ang II
Secreted CTGF
Intracellular CTGF
Tubulin
Intracellular CTGF
relative change in CTGF
Control
Control + Ang II
CCG
CCG + Ang II
Secreted CTGF
relative change in CTGF
Control
Control + Ang II
CCG
CCG + Ang II

By qPCR we could show that in 2D cultures of NRCF overexpression of p63RhoGEF led to prolonged increase of the transient CTGF transcription in the presence of Ang II, whereas downregulation of p63RhoGEF reduced the basal as well as Ang II-dependent CTGF transcription (Fig. 6). This resulted on the protein level after p63RhoGEF overexpression and knockdown in an increased and decreased amount of secreted CTGF in response to Ang II, respectively. However, the intracellular increase in CTGF induced by Ang II was not affected (Fig. 5). The dominant negative variant p63ΔN additionally inhibited the intracellular CTGF augmentation similar as Rho and ROCK inhibition as well as disruption of the actin cytoskeleton did (Figs. 5, 8). These data implies that there has to be parallel signal cascades which play a role in the regulation of CTGF. Whether this involves other direct $G_{q/11}$-dependent RhoGEFs like Kalirin or Trio [21], or is dependent on calcium signaling or calcium-dependent RhoA activation as already described for PDZ-RhoGEF has to be elucidated [38].

With respect to downstream mechanisms, it is highly likely that the integrity of the actin cytoskeleton is the most important factor which allows or regulates the translocation of transcription factors or regulators like MRTF into the nucleus. In this context, we show that p63RhoGEF increased and p63ΔN as well as C3T and fasudil decreased the Ang II-dependent activation of SRF likely via MRTF as demonstrated by the use of CCG1423 (Fig. 9). Moreover, the direct link between SRF and CTGF expression in cardiac fibroblasts was established by CCG1423 as it was already demonstrated before in LPA-treated peritoneal fibroblasts [39]. Interestingly, CCG itself increased the basal activity of SRF and of intracellular CTGF. We hypothesize that this increase is due to the inhibition of the MRTF translocation into the nucleus which might lead to more effective interaction of the SRF with other co-factors like the ETS-domain containing co-factors [40]. Moreover, the ROCK inhibitor H1152p was not effective in inhibition of the Ang II-dependent SRF activation but in reducing CTGF expression (Figs. 8, 9), thus it can be assumed that other transcription factors are involved in the regulation of CTGF. A likely candidate is the YAP/Tead complex which was proven to be important for CTGF regulation [41]. A role of RhoA/ROCK was already demonstrated in this context [42].

Even if the detailed analysis of CTGF regulation in 2D cultures argues for a complex underlying signaling, the outcome of p63RhoGEF overexpression in cardiac fibroblasts in EHM as well as in ECT is in our view compelling. Changes in p63RhoGEF expression led to similarly directed changes in CTGF expression arguing for a role of p63RhoGEF in the regulation of CTGF in tissues (Figs. 2, 3). This is further supported by their positive correlation in hearts from mice which were subjected to an increase in afterload and displaying cardiac fibrosis and hypertrophy (Fig. 1) [25].

A key finding of this manuscript is the influence of p63RhoGEF on the contractility and tissue properties of EHM and ECT. We could show that increased p63RhoGEF expression in cardiac fibroblasts led to a higher twitch and resting tension of EHM and increased stiffness of ECT. In contrast, p63ΔN decreased EHM contractility and stiffness of ECT by trend and the knockdown of p63RhoGEF clearly reduced ECT stiffness (Figs. 2; 3). Importantly, in the EHM model we found that an increase in p63RhoGEF in cardiomyocytes is not sufficient to induce similar changes (Suppl. Fig. S3). This clearly argues for a role of p63RhoGEF in auto- and paracrine function of cardiac fibroblasts. It can be assumed that the direct regulation of the expression of secreted factors as shown for CTGF is only one mechanism involved in this function. The other may rely in its potential role as a regulator of secretion processes per se. This is supported on the one hand by its main impact on extracellular CTGF in 2D cultures and on the other hand we demonstrate that in p63RhoGEF-expressing ECT the amount of CTGF is higher before stretch, but lower after stretch compared to controls (Fig. 3). This suggests that with the help of p63RhoGEF the release of secreted factors is more effective and explains the predominant change in secreted CTGF in 2D cultures (Fig. 5). So far it is not clear how p63RhoGEF interferes with the secretion machinery, but from its localization in cardiac fibroblasts at the trans-Golgi network as well as at the base of primary cilia its role as regulator of secretion is suggestive (Fig. 7).

Whether CTGF is the responsible regulating factor of tissue stiffness in this study is not clear. CTGF has been accused to be pro-fibrotic due to its consistent up-regulation in diverse fibrotic diseases [43] and thus would be a likely mediator of the observed changes in tissue stiffness. However, there is increasing conflicting data on CTGF's function in the heart. In a recent work, it was convincingly demonstrated that neither its heart-specific deletion nor its overexpression had any influence on cardiac remodeling and function with aging or after multiple stress stimuli [44]. This is in sharp contrast to other mouse studies demonstrating either a beneficial effect of CTGF for cardiomyocyte survival or a detrimental effect on cardiac fibrosis after TAC [8–11]. Thus further unbiased studies like secretome analyses have to be performed in order to identify responsible factors downstream of p63RhoGEF-RhoA explaining the observed changes in tissue properties.

Supplementary data to this article can be found online at http://dx.doi.org/10.1016/j.yjmcc.2015.09.009.

Authors' contributions

AO, SP, CMW, KN, NK, CAW, AJ, CV performed experiments with cardiac fibroblasts; SP performed the confocal imaging, MT and WHZ were involved in EHM experiments; AO, KT and GH were involved in TAC experiments; TW helped to design the study and SL designed the study and wrote the manuscript.

Conflict of Interest

The authors declare that they have no conflict of interest.

Abbreviations

Ang II	angiotensin II
C3T	C3 transferase
CSQ	calsequestrin
CTGF	connective tissue growth factor
ECT	engineered connective tissue
ECM	extracellular matrix
EGFP	enhanced green fluorescent protein
EHM	engineered heart muscle
ET-1	endothelin-1
GEF	guanine nucleotide exchange factor
NRCF	neonatal rat cardiac fibroblast
PBGD	porphobilinogen deaminase
PE	phenylephrine
SRF	serum response factor

Fig. 9. The p63RhoGEF-dependent CTGF regulation involves SRF. A) NRCFs were co-transfected with pCMV-3B (control), pCMV-p63ΔN, pCMV-p63RhoGEF, plus pSRE.L and pRL.TK, serum-starved for 24 h and treated with 100 nM Ang II for 24 h. B-C) NRCF were co-transfected with pSRE.L and pRL.TK, serum-starved for 24 h, pre-incubated with 1 μg/ml C3T (B) or 300 nM H1152p or 10 μM fasudil (C) for 30 min and treated with 100 nM Ang II for 24 h. All values are means ± SEM and ratios of firefly/renilla luciferase measurements normalized to controls, $^*p < 0.05$ vs. control, n = 4–6, measured in 4 replicates. D) NRCFs were pre-incubated 300 nM H1152p or 10 μM fasudil for 30 min and treated with 100 nM Ang II for 24 h. The actin cytoskeleton was stained with FITC-phalloidin and nuclei with DAPI, magnification 100×. E) NRCFs were co-transfected with pSRE.L and pRL.TK, serum-starved for 24 h, pre-incubated with 10 μM CCG-1423 for 1 h and treated with 100 nM Ang II for 24 h. All values are means ± SEM and ratios of firefly/renilla luciferase measurements normalized to controls, $^*p < 0.05$, n = 3, measured in 4 replicates. F) NRCFs were pre-incubated with 10 μM CCG-1423 for 1 h and treated with 100 nM Ang II for 24 h. The actin cytoskeleton was stained with FITC-phalloidin and nuclei with DAPI, magnification 100×. G) NRCFs were pre-incubated with 10 μM CCG-1423 for 1 h and treated with 100 nM Ang II for 24 h. The amounts of intracellular and secreted CTGF were determined by immunoblot analyses of cell lysates and conditioned media. Representative immunoblots are shown. All values are given as means ± SEM, normalized to tubulin and relative to control, $^*p < 0.05$ vs. control, n = 5.

TAC	transversal aortic constriction
TGF-β	transforming growth factor-β
WGA	wheat germ agglutinin

Acknowledgments

The authors thank K. Schenk, B. Ramba as well as the SFB 1002 service project (TP S) for technical assistance. We further thank Prof. Ali El-Armouche for his contribution to the animal studies. We also like to thank Prof. B. Schwappach for sharing GOPC and Lamp2 antibodies with us. Sources of Funding: This work was supported by German Research Council grants Lu1486/1-1 (to SL and TW), SFB 1002 (to SL (TPC02), KT (TPB04), GH (TPB04) and WHZ (TPC04)) and IRTG1816 (to AO). WHZ was further supported by grants from the German Research Council (DFG ZI 708/7-1, 8-1, 10–1, SFB 937 A18), the German Federal Ministry for Science and Education (DZHK, 13GW0007A), and the National Institutes of Health (U01 HL099997). NK was funded by the German Academic Exchange Service (DAAD).

References

[1] I. Manabe, T. Shindo, R. Nagai, Gene expression in fibroblasts and fibrosis: involvement in cardiac hypertrophy, Circ. Res. 91 (2002) 1103–1113.
[2] B. Swynghedauw, Molecular mechanisms of myocardial remodeling, Physiol. Rev. 79 (1999) 215–262.
[3] N.L. Thompson, F. Bazoberry, E.H. Speir, W. Casscells, V.J. Ferrans, K.C. Flanders, et al., Transforming growth factor beta-1 in acute myocardial infarction in rats, Growth Factors 1 (1988) 91–99.
[4] N. Takahashi, A. Calderone, N.J. Izzo Jr., T.M. Maki, J.D. Marsh, W.S. Colucci, Hypertrophic stimuli induce transforming growth factor-beta 1 expression in rat ventricular myocytes, J. Clin. Invest. 94 (1994) 1470–1476.
[5] J.G. Abreu, N.I. Ketpura, B. Reversade, E.M. De Robertis, Connective-tissue growth factor (CTGF) modulates cell signalling by BMP and TGF-beta, Nat. Cell Biol. 4 (2002) 599–604.
[6] A. Daniels, M. van Bilsen, R. Goldschmeding, G.J. van der Vusse, F.A. van Nieuwenhoven, Connective tissue growth factor and cardiac fibrosis, Acta Physiol. (Oxf.) 195 (2009) 321–338.
[7] D.M. Bradham, A. Igarashi, R.L. Potter, G.R. Grotendorst, Connective tissue growth factor: a cysteine-rich mitogen secreted by human vascular endothelial cells is related to the SRC-induced immediate early gene product CEF-10, J. Cell Biol. 114 (1991) 1285–1294.
[8] X. Zhao, E.Y. Ding, O.M. Yu, S.Y. Xiang, V.P. Tan-Sah, B.S. Yung, et al., Induction of the matricellular protein CCN1 through RhoA and MRTF-a contributes to ischemic cardioprotection, J. Mol. Cell. Cardiol. 75 (2014) 152–161.
[9] A.N. Panek, M.G. Posch, N. Alenina, S.K. Ghadge, B. Erdmann, E. Popova, et al., Connective tissue growth factor overexpression in cardiomyocytes promotes cardiac hypertrophy and protection against pressure overload, PLoS ONE 4 (2009) e6743.
[10] I.T. Moe, T.A. Pham, E.M. Hagelin, M.S. Ahmed, H. Attramadal, CCN2 exerts direct cytoprotective actions in adult cardiac myocytes by activation of the PI3-kinase/Akt/GSK-3beta signaling pathway, J. Cell Commun. Signal. 7 (2013) 31–47.
[11] M.S. Ahmed, J. Gravning, V.N. Martinov, T.G. von Lueder, T. Edvardsen, G. Czibik, et al., Mechanisms of novel cardioprotective functions of CCN2/CTGF in myocardial ischemia–reperfusion injury, Am. J. Physiol. Heart Circ. Physiol. 300 (2011) H1291–H1302.
[12] M. Ruperez, O. Lorenzo, L.M. Blanco-Colio, V. Esteban, J. Egido, M. Ruiz-Ortega, Connective tissue growth factor is a mediator of angiotensin II-induced fibrosis, Circulation 108 (2003) 1499–1505.
[13] S.W. Xu, S.L. Howat, E.A. Renzoni, A. Holmes, J.D. Pearson, M.R. Dashwood, et al., Endothelin-1 induces expression of matrix-associated genes in lung fibroblasts through MEK/ERK, J. Biol. Chem. 279 (2004) 23098–23103.
[14] J. Rodriguez-Vita, M. Ruiz-Ortega, M. Ruperez, V. Esteban, E. Sanchez-Lopez, J.J. Plaza, et al., Endothelin-1, via ETA receptor and independently of transforming growth factor-beta, increases the connective tissue growth factor in vascular smooth muscle cells, Circ. Res. 97 (2005) 125–134.
[15] A.G. Recchia, E. Filice, D. Pellegrino, A. Dobrina, M.C. Cerra, M. Maggiolini, Endothelin-1 induces connective tissue growth factor expression in cardiomyocytes, J. Mol. Cell. Cardiol. 46 (2009) 352–359.
[16] M.S. Ahmed, E. Oie, L.E. Vinge, A. Yndestad, G. Oystein Andersen, Y. Andersson, et al., Connective tissue growth factor—a novel mediator of angiotensin II-stimulated cardiac fibroblast activation in heart failure in rats, J. Mol. Cell. Cardiol. 36 (2004) 393–404.
[17] D. Lavall, C. Selzer, P. Schuster, M. Lenski, O. Adam, H.J. Schafers, et al., The mineralocorticoid receptor promotes fibrotic remodeling in atrial fibrillation, J. Biol. Chem. 289 (2014) 6656–6668.
[18] M. Touvron, B. Escoubet, M. Mericskay, A. Angelini, L. Lamotte, M.P. Santini, et al., Locally expressed IGF1 propeptide improves mouse heart function in induced dilated cardiomyopathy by blocking myocardial fibrosis and SRF-dependent CTGF induction, Dis. Model. Mech. 5 (2012) 481–491.
[19] M. Souchet, E. Portales-Casamar, D. Mazurais, S. Schmidt, I. Leger, J.L. Javre, et al., Human p63RhoGEF, a novel RhoA-specific guanine nucleotide exchange factor, is localized in cardiac sarcomere, J. Cell Sci. 115 (2002) 629–640.
[20] S. Lutz, A. Freichel-Blomquist, Y. Yang, U. Rumenapp, K.H. Jakobs, M. Schmidt, et al., The guanine nucleotide exchange factor p63RhoGEF, a specific link between Gq/11-coupled receptor signaling and RhoA, J. Biol. Chem. 280 (2005) 11134–11139.
[21] S. Lutz, A. Shankaranarayanan, C. Coco, M. Ridilla, M.R. Nance, C. Vettel, et al., Structure of Galphaq-p63RhoGEF-RhoA complex reveals a pathway for the activation of RhoA by GPCRs, Science 318 (2007) 1923–1927.
[22] C.M. Wuertz, A. Lorincz, C. Vettel, M.A. Thomas, T. Wieland, S. Lutz, p63RhoGEF–a key mediator of angiotensin II-dependent signaling and processes in vascular smooth muscle cells, FASEB J. 24 (2010) 4865–4876.
[23] K. Momotani, M.V. Artamonov, D. Utepbergenov, U. Derewenda, Z.S. Derewenda, A.V. Somlyo, p63RhoGEF couples Galpha(q/11)-mediated signaling to Ca2+ sensitization of vascular smooth muscle contractility, Circ. Res. 109 (2011) 993–1002.
[24] P. Camelliti, T.K. Borg, P. Kohl, Structural and functional characterisation of cardiac fibroblasts, Cardiovasc. Res. 65 (2005) 40–51.
[25] K. Toischer, A.G. Rokita, B. Unsold, W. Zhu, G. Kararigas, S. Sossalla, et al., Differential cardiac remodeling in preload versus afterload, Circulation 122 (2010) 993–1003.
[26] T.C. He, S. Zhou, L.T. da Costa, J. Yu, K.W. Kinzler, B. Vogelstein, A simplified system for generating recombinant adenoviruses, Proc. Natl. Acad. Sci. U. S. A. 95 (1998) 2509–2514.
[27] F. Cuello, S.C. Bardswell, R.S. Haworth, X. Yin, S. Lutz, T. Wieland, et al., Protein kinase D selectively targets cardiac troponin I and regulates myofilament Ca2+ sensitivity in ventricular myocytes, Circ. Res. 100 (2007) 864–873.
[28] K.A. Webster, D.J. Discher, N.H. Bishopric, Induction and nuclear accumulation of fos and jun proto-oncogenes in hypoxic cardiac myocytes, J. Biol. Chem. 268 (1993) 16852–16858.
[29] W.H. Zimmermann, C. Fink, D. Kralisch, U. Remmers, J. Weil, T. Eschenhagen, Three-dimensional engineered heart tissue from neonatal rat cardiac myocytes, Biotechnol. Bioeng. 68 (2000) 106–114.
[30] W.H. Zimmermann, K. Schneiderbanger, P. Schubert, M. Didie, F. Munzel, J.F. Heubach, et al., Tissue engineering of a differentiated cardiac muscle construct, Circ. Res. 90 (2002) 223–230.
[31] S. Lutz, A. Freichel-Blomquist, U. Rumenapp, M. Schmidt, K.H. Jakobs, T. Wieland, p63RhoGEF and GEFT are Rho-specific guanine nucleotide exchange factors encoded by the same gene, Naunyn Schmiedeberg's Arch. Pharmacol. 369 (2004) 540–546.
[32] J. Mao, H. Yuan, W. Xie, D. Wu, Guanine nucleotide exchange factor GEF115 specifically mediates activation of Rho and serum response factor by the G protein alpha subunit Galpha13, Proc. Natl. Acad. Sci. U. S. A. 95 (1998) 12973–12976.
[33] M.D. Hains, D.P. Siderovski, T.K. Harden, Application of RGS box proteins to evaluate G-protein selectivity in receptor-promoted signaling, Methods Enzymol. 389 (2004) 71–88.
[34] D. Huang, Y. Wang, C. Yang, Y. Liao, K. Huang, Angiotensin II promotes poly(ADP-ribosyl)ation of c-Jun/c-Fos in cardiac fibroblasts, J. Mol. Cell. Cardiol. 46 (2009) 25–32.
[35] K. Tiede, K. Stoter, C. Petrik, W.B. Chen, H. Ungefroren, M.L. Kruse, et al., Angiotensin II AT(1)-receptor induces biglycan in neonatal cardiac fibroblasts via autocrine release of TGFbeta in vitro, Cardiovasc. Res. 60 (2003) 538–546.
[36] S. Muehlich, I. Cicha, C.D. Garlichs, B. Krueger, G. Posern, M. Goppelt-Struebe, Actin-dependent regulation of connective tissue growth factor, Am. J. Physiol. Cell Physiol. 292 (2007) C1732–C1738.
[37] T. Morita, T. Mayanagi, K. Sobue, Reorganization of the actin cytoskeleton via transcriptional regulation of cytoskeletal/focal adhesion genes by myocardin-related transcription factors (MRTFs/MAL/MKLs), Exp. Cell Res. 313 (2007) 3432–3445.
[38] Z. Ying, F.R. Giachini, R.C. Tostes, R.C. Webb, PYK2/PDZ-RhoGEF links Ca2+ signaling to RhoA, Arterioscler. Thromb. Vasc. Biol. 29 (2009) 1657–1663.
[39] N. Sakai, J. Chun, J.S. Duffield, T. Wada, A.D. Luster, A.M. Tager, LPA1-induced cytoskeleton reorganization drives fibrosis through CTGF-dependent fibroblast proliferation, FASEB J. 27 (2013) 1830–1846.
[40] C. Esnault, A. Stewart, F. Gualdrini, P. East, S. Horswell, N. Matthews, et al., Rho-actin signaling to the MRTF coactivators dominates the immediate transcriptional response to serum in fibroblasts, Genes Dev. 28 (2014) 943–958.
[41] A.V. Pobbati, W. Hong, Emerging roles of TEAD transcription factors and its coactivators in cancers, Cancer Biol. Ther. 14 (2013) 390–398.
[42] H. Cai, Y. Xu, The role of LPA and YAP signaling in long-term migration of human ovarian cancer cells, Cell Commun. Signal. CCS 11 (2013) 31.
[43] X. Shi-Wen, A. Leask, D. Abraham, Regulation and function of connective tissue growth factor/CCN2 in tissue repair, scarring and fibrosis, Cytokine Growth Factor Rev. 19 (2008) 133–144.
[44] F. Accornero, J.H. van Berlo, R.N. Correll, J.W. Elrod, M.A. Sargent, A. York, et al., Genetic analysis of connective tissue growth factor as an effector of transforming growth factor beta signaling and cardiac remodeling, Mol. Cell. Biol. 35 (2015) 2154–2164.